ISSN 0973-8975
J.Mech.Cont.& Math. Sci., Vol.-9, No.-1, July (2014) Pages 1278-1291

PRESSURE-DRIVEN FLOW INSTABILITY WITH CONVECTIVE HEAT TRANSFER THROUGH A ROTATING CURVED CHANNEL WITH RECTANGULAR CROSS-SECTION: THE CASE OF NEGATIVE ROTATION

By

[1]Md. Zohurul Islam[*], [2]Md. Sirajul Islam, [3]Muhammad Minarul Islam

[1]Department of Mathematics, Jessore shikkha Board Model School and College, Jessore-7401, Bangladesh

[2] Mathematics Department, Bangabandhu SheikhMujibur Rahmain Science and Technology University, Gopalganj-8100, Bangladesh

Abstract:

Due to engineering applications and its intricacy, the flow in a rotating curved duct has become one of the most challenging research fields of fluid mechanics. A comprehensive numerical study is presented for the fully developed two-dimensional thermal flow of viscous incompressible fluid through a rotating curved rectangular duct of constant curvature $\delta = 0.1$. *Numerical calculations are carried out by using a spectral method and covering a wide range of the Taylor number* $-2000 \le Tr < 0$ *and the Dean number* $100 \le Dn \le 1000$ *for the constant Grashof number* $Gr = 100$. *A temperature difference is applied, that is the outer wall of the duct is heated while the inner wall is cooled. The rotation of the duct about the center of curvature is imposed, and the effects of rotation (Coriolis force) on the unsteady flow characteristics are investigated. Flow characteristics are investigated for the case of negative duct rotation. We investigate the unsteady flow characteristics for the Taylor number* $-2000 \le Tr < 0$ *and it is found that the unsteady flow undergoes in the scenario 'steady-state→ periodic→ multi-periodic → steady-state', if Tr is increased in the negative direction. Contours of secondary flow patterns and temperature profiles are also obtained at several values of Tr, and it is found that there exist two- and multi-vortex solutions if the duct rotation is involved in the negative direction.*

Keywords and phrases : thermal flow, viscous incompressible fluid, duct rotation, Taylor number, Grashof number

বিমূর্ত সার ***(Bengali version of the Abstract)***

ইঞ্জিনিয়ারিং - এ প্রয়োগ এবং ইহার জটিলতার জন্য একটি ঘূর্ণায়মান বক্রনলীতে প্রবাহটি ফ্লুয়িড বলবিদ্যার একটি অন্যতম চ্যালেঞ্জ ধর্মী গবেষণার ক্ষেত্রে পরিণত হয়েছে । $\delta = 0.1$ ধ্রুবক

বক্রতা বিশিষ্ট একটি ঘূর্ণায়মান বক্র আয়তকার নলীর ভিতর দিয়ে সান্দ্র অসংনম্য ফ্লুয়িডের পূর্ণ বৃদ্ধিপ্রাপ্ত দ্বিমাত্রিক তাপীয় প্রবাহের জন্য একটি ব্যাপক সাংখ্য অনুসন্ধান উপস্থাপন করা হয়েছে । বর্ণালীয় পদ্ধতিকে ব্যবহার করে সাংখ্য গণনা সম্পাদন করা হয়েছে এবং ধ্রুবক গ্রাশফ্ সংখ্যা (Grashof number) $Gr = 100$ *এর জন্য টেলার নাম্বার (Taylor number)* $-2000 \le Tr < 0$ *এবং ডীন নাম্বার (Dean number)* $100 \le Dn \le 1000$ *এর দীর্ঘ্য পাল্লাকে অর্ন্তভুক্ত করা হয়েছে । উষ্ণতার পার্থক্যকে প্রয়োগ করা হয়েছে, অর্থাৎ নলীর বাইরের প্রাচীরকে উত্তপ্ত করা হয়েছে যখন ভিতরের প্রাচীরকে ঠান্ডা রাখা হয়েছে । নলীর ঘূর্ণন - বক্রতা কেন্দ্রে আরোপ করা হয়েছে । টলটলায়মান প্রবাহ বৈশিষ্ট্যের উপর আবর্তনের প্রভাব (Coriolis force) কে অনুসন্ধান করা হয়েছে ।* $-2000 \le Tr < 0$ *টেলর নাম্বারের জন্য টলটলায়মান প্রবাহের বৈশিষ্ট্যকে আমরা অনুসন্ধান করেছি এবং এটা দেখা গেছে যে টলটলায়মান প্রবাহটির চিত্রকল্পটই এইরূপ ঃ ''স্থায়ী অবস্থা --- পর্যাবৃত্ত -- বহু পর্যাবৃত্ত -- স্থায়ী অবস্থা''। যদি ঋণাত্মক দিকে Tr - এর মান বাড়ানো হয় দ্বিতীয় শ্রেণীর প্রবাহ নমুনার কনটুর (Contour) এবং উষ্ণতার পার্শ্বচিত্রকে Tr - এর বহুবিধ মানে নির্ণয় করা হয় এবং এটাও দেখা গেছে যে দুই এবং বহু - আবর্ত সমাধান বিদ্যমান থাকে যদি নলীর আবর্তন ঋণাত্মক দিকের সঙ্গে বিজাড়িত হয় ।*

1. Introduction:

The study of flow and heat transfer in a curved ducts and channels has attracted considerable attention because of their ample applications in fluids engineering. Due to engineering applications and their intricacy, the flow in a rotating curved duct has become one of the most challenging research fields of fluid mechanics. Since rotating machines were introduced into engineering applications, such as rotating systems, gas turbines, electric generators, heat exchangers, cooling system and some separation processes, scientists have paid considerable attention to study rotating curved duct flows. The readers are referred to Nandakumar and Masliyah [1], Ito [2] and Yanase *et al.* [3] for some outstanding reviews on curved duct flows.

The fluid flowing in a rotating curved duct is subjected to two forces: the *Coriolis force* due to rotation and the *centrifugal force* due to curvature. For isothermal flows of a constant property fluid, the Coriolis force tends to produce vortices while centrifugal force is purely hydrostatic. When a temperature induced variation of fluid density occurs for non-isothermal flows, both Coriolis and centrifugal type buoyancy forces can contribute to the generation of vortices. These two effects of rotation either enhance or counteract each other in a non-linear manner depending on the direction of wall heat flux and the flow domain. Therefore, the effect of system rotation is more subtle and complicated and yields new; richer features of flow and heat transfer in general, bifurcation and stability in particular, for non-isothermal flows. Selmi *et al.* [4] examined the combined effects of system rotation and curvature on the bifurcation structure of two-dimensional flows in a rotating curved duct with square cross section. Wang and Cheng [5], employing finite volume method, examined the flow characteristics and heat transfer in curved square ducts for positive rotation and found reverse secondary flow for the co-rotation cases. Selmi and Nandakumer [6] and Yamamoto *et al*. [7] performed studies on the flow in a rotating curved rectangular duct. When a temperature induced variation of fluid density occurs for non-isothermal flows, both Coriolis and centrifugal type buoyancy forces can contribute to the generation of vorticity (Mondal *et. al.*, [8]). These two effects of rotation either enhance or counteract each other in a non-linear manner depending on the direction of wall heat flux and the flow domain. Therefore, the effect of system rotation is more subtle and complicated and yields new; richer features of flow and heat transfer in general, bifurcation and stability in particular, for non-isothermal flows. Very recently, Mondal *et al.* [9], [10] and [11] performed numerical investigation of the non-isothermal flows through a rotating curved square rectangular duct and obtained substantial results. However, there is no known study on rotating curved rectangular duct flows with buoyancy effect. The present paper is, therefore, an attempt to fill up this gap. Studying the effects of rotation

on the flow characteristics, caused by the buoyancy forces with pressure dropped, is an important objective of the present study.

2. PHYSICAL MODEL

Consider a hydro-dynamically and thermally fully developed two-dimensional flow of viscous incompressible fluid through a rotating curved duct with rectangular cross section, whose height and wide are *2h* and *2l* respectively. The coordinate system with the relevant notation is shown in Fig. 1, where x' and y' axes are taken to be in the horizontal and vertical directions respectively and *z'* is the axial direction. The system

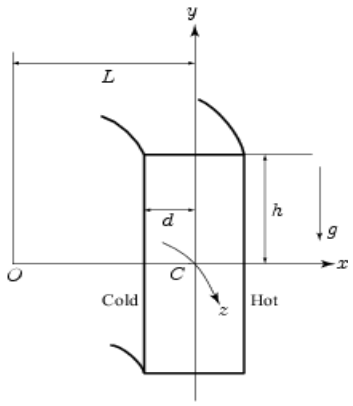

rotates at a constant angular velocity Ω_T around the y' axis. It is assumed that the outer wall of the duct is heated while the inner wall is cooled. The temperature of the outer wall is $T_0 + \Delta T$ and that of the inner wall is $T_0 - \Delta T$, where $\Delta T > 0$. The *x, y,* and *z* axes are taken to be in the horizontal, vertical, and axial directions respectively. It is assumed that the flow is uniform in the axial direction, which is driven by a constant pressure gradient *G* along the center-line of the duct as shown in Fig. 1. The variables are non-dimensionalized by using the representative length l and the representative velocity U_0 .

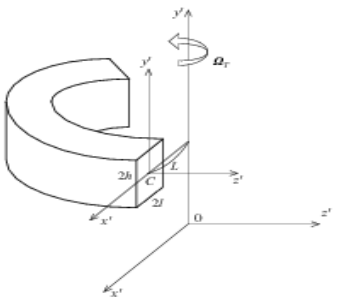

Fig. 1: Coordinate system of the rotating duct and physical configuration of the system.

3. MATHEMATICAL MODEL

Since the flow field is uniform in the z direction, the sectional stream function ψ is introduced as,

$$u = \frac{1}{1+\delta x}\frac{\partial \psi}{\partial y}, \quad v = -\frac{1}{1+\delta x}\frac{\partial \psi}{\partial x}. \tag{1}$$

A new coordinate variable y' is introduced in the y direction as $y = ay'$, where $a = h/d$ is the aspect ratio of the duct cross-section. From now on y denotes y' for the sake of simplicity. Then the basic equations for the axial velocity *w*, the stream function ψ and the temperature T are derived from the Navier-Stokes equations and the energy equation under the *Boussinesq approximation* as,

$$(1+\delta x)\frac{\partial w}{\partial t} + \frac{1}{a}\frac{\partial(w,\psi)}{\partial(x,y)} - Dn + \frac{\delta^2 w}{1+\delta x} = (1+\delta x)\Delta_2 w - \frac{1}{a}\frac{\delta}{(1+\delta x)}\frac{\partial \psi}{\partial y}w + \delta\frac{\partial w}{\partial x} - \delta Tr\frac{\partial \psi}{\partial y} \tag{2}$$

$$\left(\Delta_2 - \frac{\delta}{1+\delta x}\frac{\partial}{\partial x}\right)\frac{\partial \psi}{\partial t} = -\frac{1}{a}\frac{1}{(1+\delta x)}\frac{\partial(\Delta_2\psi,\psi)}{\partial(x,y)} + \frac{1}{a}\frac{\delta}{(1+\delta x)^2}\times\left[\frac{\partial \psi}{\partial y}\left(2\Delta_2\psi - \frac{3\delta}{1+\delta x}\frac{\partial \psi}{\partial x} + \frac{\partial^2 \psi}{\partial x^2}\right)\right.$$

$$\left. - \frac{\partial \psi}{\partial x}\frac{\partial^2 \psi}{\partial x \partial y}\right] + \frac{\delta}{(1+\delta x)^2}\times\left[3\delta\frac{\delta^2 \psi}{\partial x^2} - \frac{3\delta^2}{1+\delta x}\frac{\partial \psi}{\partial x}\right] - \frac{2\delta}{1+\delta x}\frac{\partial}{\partial x}\Delta_2\psi + \frac{1}{a}w\frac{\partial w}{\partial y} + \Delta_2^2\psi$$

$$-Gr(1+\delta x)\frac{\partial T}{\partial x} - \frac{1}{2}Tr\frac{\partial w}{\partial y}, \tag{3}$$

$$\frac{\partial T}{\partial t} + \frac{1}{(1+\delta x)}\frac{\partial(T,\psi)}{\partial(x,y)} = \frac{1}{\Pr}\left(\Delta_2 T + \frac{\delta}{1+\delta x}\frac{\partial T}{\partial x}\right) \tag{4}$$

where, $\Delta_2 \equiv \frac{\partial^2}{\partial x^2} + \frac{1}{a^2}\frac{\partial^2}{\partial y^2}$, $\frac{\partial(f,g)}{\partial(x,y)} \equiv \frac{\partial f}{\partial x}\frac{\partial g}{\partial y} - \frac{\partial f}{\partial y}\frac{\partial g}{\partial x}$

The non-dimensional parameters Dn, the Dean number, Tr, the Taylor number, *Gr*, the Grashof number and *Pr*, the prandtl number, which appear in equations (2) to (4) are defined as:

$$Dn = \frac{Gl^3}{\mu\upsilon}\sqrt{\frac{2l}{L}}, \quad Tr = \frac{2\sqrt{2\delta}\Omega_T l^3}{\upsilon\delta}, \quad Gr = \frac{\beta g \Delta T l^3}{\upsilon^2}, \quad \Pr = \frac{\upsilon}{\kappa} \tag{5}$$

Where

μ, β, κ and g are the viscosity, the coefficient of thermal expansion, the co-efficient of thermal diffusivity and the gravitational acceleration respectively, υ is the viscosity of the fluid. In the present study, *Dn* and *Tr* are varied while *Gr*, a, δ and Pr are fixed as *Gr* =100, $a = 2.0$, $\delta = 0.1$ and $\mathrm{Pr} = 7.0$ (water).

Boundary conditions

The boundary conditions of the present study are described as follows.

The rigid boundary conditions for *w* and ψ are used as

$$w(\pm 1, y) = w(x, \pm 1) = \psi(\pm 1, y) = \psi(x, \pm 1) = \frac{\partial \psi}{\partial x}(\pm 1, y) = \frac{\partial \psi}{\partial y}(x, \pm 1) = 0 \tag{6}$$

and the temperature T is assumed to be constant on the walls as

$$T(1, y) = 1, \quad T(-1, y) = -1, \quad T(x, \pm 1) = x \tag{7}$$

4. NUMERICAL PROCEDURE

In order to solve the Equations (2) to (4) numerically, the spectral method is used. By this method the expansion functions $\phi_n(x)$ and $\psi_n(x)$ are expressed as

$$\left.\begin{aligned} \phi_n(x) &= (1 - x^2) C_n(x), \\ \psi_n(x) &= (1 - x^2)^2 C_n(x) \end{aligned}\right\} \tag{8}$$

where $C_n(x) = \cos\left(n \cos^{-1}(x)\right)$ is the n^{th} order Chebyshev polynomial. $w(x, y, t)$, $\psi(x, y, t)$ and $T(x, y, t)$ are expanded in terms of the expansion functions $\phi_n(x)$ and $\psi_n(x)$ as

$$\left.\begin{aligned} w(x, y, t) &= \sum_{m=0}^{M} \sum_{n=0}^{N} w_{m\,n}(t) \varphi_m(x) \varphi_n(y) \\ \psi(x, y, t) &= \sum_{m=0}^{M} \sum_{n=0}^{N} \psi_{m\,n}(t) \psi_m(x) \psi_n(y). \\ T(x, , y, t) &= \sum_{m=0}^{M} \sum_{n=0}^{N} T_{m\,n}\, \varphi_m(x) \varphi_n(y) + x \end{aligned}\right\} \tag{9}$$

where M and N are the truncation numbers in the x and y directions respectively.

5. GRID SENSITIVITY TEST

The accuracy of the numerical calculations is investigated for the truncation numbers M and N used in this study. Five types of grid sizes were used to check the dependence of grid size (i.e. M and N). For good accuracy of the solutions, N is chosen equal to $2M$. The grid sizes are taken as $14\times 28,\ 16\times 32, 18\times 36, 20\times 40, 22\times 44$, and it is found that M = 16 and N = 32 give sufficient accuracy of the numerical solutions, which are not shown here for brevity. In order to calculate the unsteady solutions, the Crank-Nicolson and Adams-Bashforth methods together with the function expansion (9) and the collocation methods are applied to Eqs. (2) to (4).

4. Resistance coefficient

We use the resistance coefficient λ as one of the representative quantities of the flow state. It is also called the *hydraulic resistance coefficient*, and is generally used in fluids engineering, defined as

$$\frac{P_1^* - P_2^*}{\Delta z^*} = \frac{\lambda}{dh^*}\frac{1}{2}\rho\left\langle w^* \right\rangle^2, \tag{10}$$

where quantities with an asterisk denote the dimensional ones, $\langle\,\rangle$ stands for the mean over the cross section of the rectangular duct, and $d_h^* = 4(2l\times 4lh)/(4l\times 8lh)$. Since $\left(P_1^* - P_2^*\right)/\Delta z^* = G$, λ is related to the mean non-dimensional axial velocity $\langle w\rangle$ as

$$\lambda = \frac{16\sqrt{2\delta}\,Dn}{3\langle w\rangle^2}, \tag{11}$$

where $\langle w\rangle = \sqrt{2\delta}\,d/\nu\left\langle w^* \right\rangle$. In this paper, λ is used to calculate the unsteady solutions by numerical computations.

7. RESULTS

We take a curved rectangular channel of aspect ratio $a = 2.0$ and curvature $\delta = 0.1$ and rotate it around the centre of curvature with an angular velocity Ω_T in the negative direction. In this paper, time evolution calculations of the resistant coefficient λ are performed for the non-isothermal flows (Gr = 100) over a wide range of the Dean

Numbers (*Dn*) and the Taylor Number (*Tr*) for the two cases of the duct rotation, *Case I*: *Dn* = 500 and *Case II*: *Dn* = 800.

5.1 *Case I*: Dean Number, *Dn*=500

For negative rotation we perform time evolution of λ for $-2000 \le Tr < 0$ and $100 \le Dn \le 1000$. Figure 2(a) shows time evolution of λ for Tr = -100 and Dn = 500 at Gr = 100. It is found that the unsteady flow at Tr = -100 is a steady state solution. Fig. 2(b) shows typical contours of secondary flow patterns and temperature profiles for Tr = -100 and Dn = 500, where we find that the unsteady flow is a two -vortex solution. This is caused by the combined action of the Coriolis force due to rotation and centrifugal force due to curvature, which increased the number of secondary vortices (Wang and Cheng [5]). Then we perform time evolution of λ for Tr = -360 as shown in Fig. 3(a). It is found that the unsteady flow is a multi-periodic solution. In order to observe the multi-periodic oscillation more clearly, we draw the phase space of the time evolution, result as shown in Fig. 3(b), and it is found that the flow oscillates in a definite regular pattern, which confirms that the flow is multi-periodic in the same orbit. Typical contours of secondary flow patterns and temperature profiles are shown in Fig. 3(c), which is consistent with the multi-periodic oscillations and we see that the unsteady flow generates two-vortex solution. Then we perform time evolution of λ for Tr = -640 as shown in Fig. 4(a). It is found that the unsteady flow at Tr = -640 is a weak chaotic solution, which is well justified by drawing the phase space as shown in Fig. 4(b). As seen in Fig. 4(b), the flow creates multiple orbits in its path, so that the unsteady flow at Tr = -640 is a weak chaotic solution. Typical contours of secondary flow patterns and temperature profiles for the corresponding flow parameters are shown in Fig. 4(c), where it is found that the multi-periodic to chaos oscillation at Tr = -640 is a two-vortex solution. If the rotational speed is increases more in the negative direction, for example Tr = -700 up to -2000, it is found that the flow becomes strongly chaotic which is not shown for brevity.

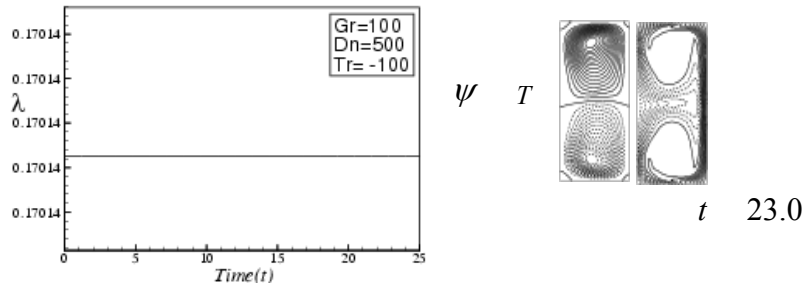

Figure 2: (a) Time evolution of λ for Dn = 500 and Tr = -100. (b) Contours of secondary flow patterns (top) and temperature profiles (bottom) for Tr = -100, at time $t = 23.0$

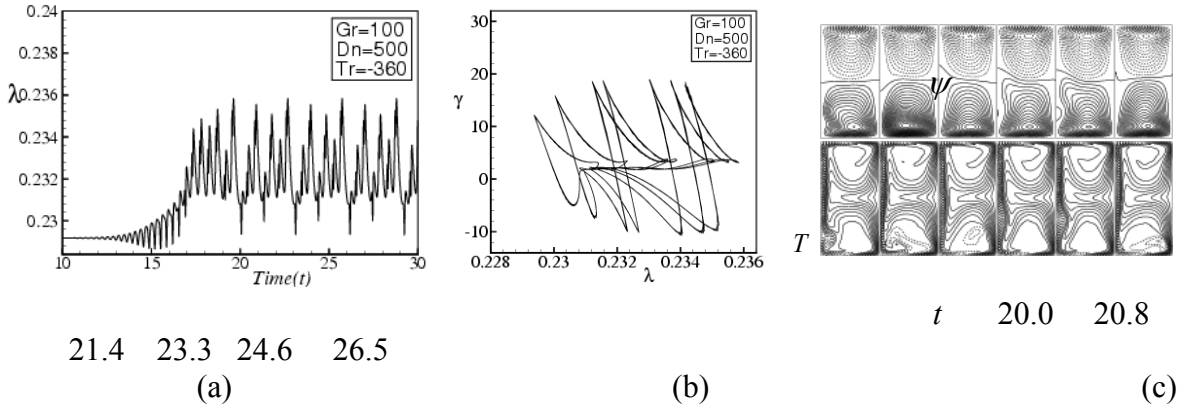

Figure 3: (a) Time evolution of λ for Dn = 500 and Tr = -360. (b) Phase space for Tr =-360, (c) Contours of secondary flow patterns (top) and temperature profiles (bottom) for Tr = -360, at time $20.0 \le t \le 26.5$.

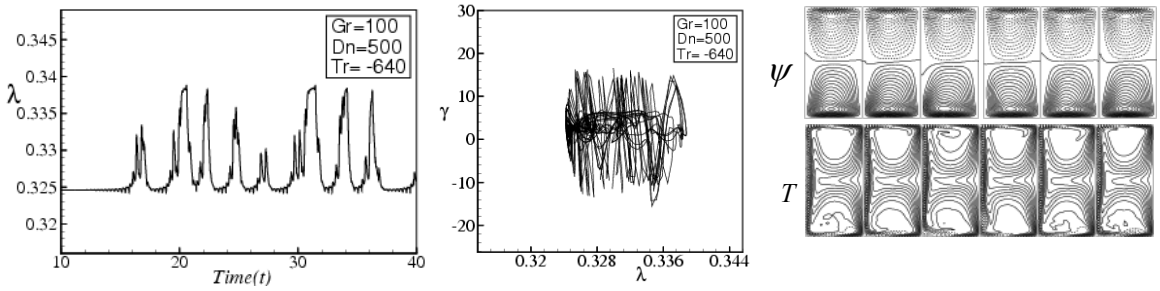

t 15.7 18.8 23.9 26.1 29.0 32.8

(a) (b) (c)

Figure 4: (a) Time evolution of λ for Dn = 500 and Tr = - 640. (b) Phase space for Tr = - 640, (c) Contours of secondary flow patterns and temperature profiles for Tr = - 640, at time $15.7 \le t \le 32.8$.

5.2 *Case II*: Dean Number, *Dn*=800

We perform time evolution of λ for $-2000 \le Tr < 0$ and $Dn = 800$ for $\delta = 0.1$. Figure 5(a) shows time evolution of λ for Dn = 800 and Tr = -100 at Gr = 100. It is found that the unsteady flow at Tr = -100 is a strongly chaotic solution, which is well justified by drawing the phase spaces as shown in Fig. 5(b). Figure 5(c) shows typical contours of secondary flow patterns and temperature profiles for Tr = - 100, where we find that flow is a four-vortex solutions. Then we perform time evolution of λ for Tr = -300 and presented in Fig.6 (a). It is found that the unsteady flow is multi-periodic oscillation at Tr = -300. The multi-periodic oscillations are well justified by depicting the phase spaces as shown in Fig. 6(b) for Tr = -300. Typical contours of secondary flow patterns and temperature profiles are shown in Figs. 6(c) for Tr = -300, which is produced four-vortex solutions. Then we perform time evolution of λ for Tr = - 400 as shown in Fig. 7(a). It is found that the unsteady flow is also a multi-periodic solution which turns into chaos. In order to observe the multi-periodic oscillation more clearly, we draw the phase space of the time evolution result as shown in Fig. 7(b) and it is found that the flow is multi-periodic. Typical contours of secondary flow patterns and temperature profiles are shown in Fig. 7(c) and we see that the unsteady flow is only two-vortex solutions. If the rotational speed is increased more, for example Tr = -500 or more up to -2000, it is found that the flow becomes chaotic. Figure 8(a) shows time evolution of λ for Tr = -500 and Dn = 800, and it is found that the flow is chaotic for all the cases. Then we draw the phase space for observing flow pattern. From the fig. 8(b) it is clear

that the flow patterns are changing multi-periodic to chaos. And finally we draw the typical contours of secondary flow patterns and temperature profile is shown in Fig. 8(b) for Tr = -500 and Dn = 800, and it is found that the unsteady flow is an asymmetric four-vortex solution. In this study, it is found that combined action of the coriolis and centrifugal force help to increase the number of secondary vortices. It is also found that, as the flow becomes chaotic, the secondary flow increases and gets stronger and consequently heat is transferred substantially outer wall of the duct.

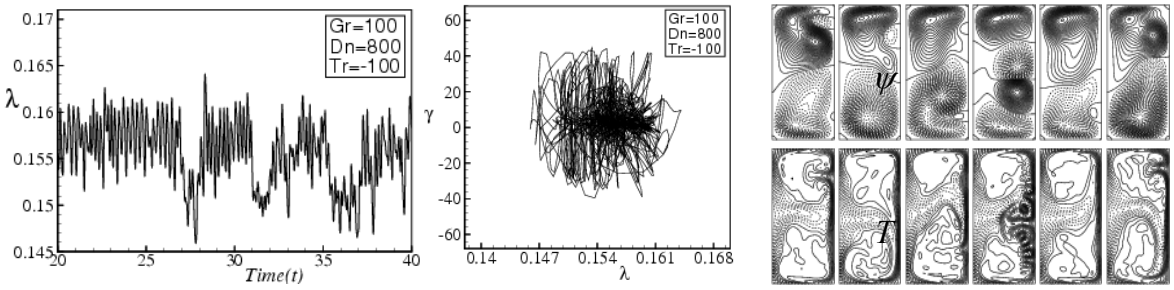

(a) **(b)** *t*

27.0 28.0 29.0 30.0 31.0 32.0

Figure 5: (a) Time evolution of λ for Tr = -100 and Dn=800, (b) Phase space for Tr = -100 (c) Contours of secondary flow patterns and temperature profiles for Tr = -100, at time $27.00 \le t \le 32.00$.

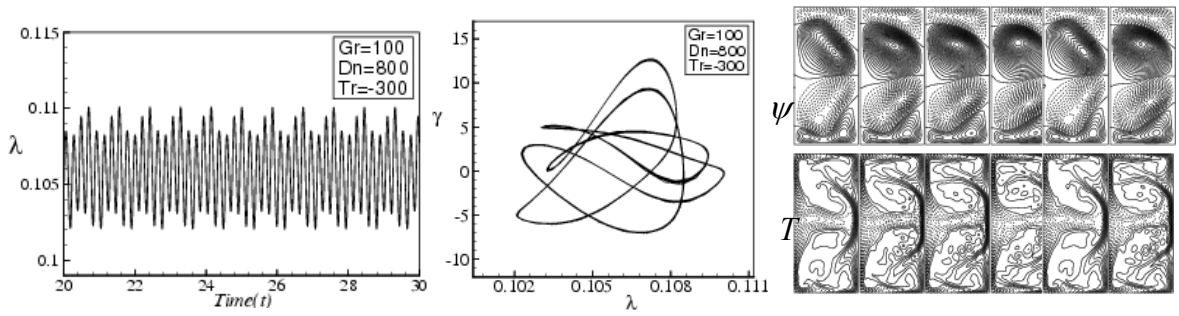

t 21.0 21.9 22.8 23.6 24.5 25.4

(a) (b) (c)

Figure 6: (a) Time evolution of λ for Tr = -300 and Dn = 800 at Gr = 100. (b) Phase space for Tr = - 300. (c) Contours of secondary flow patterns (top) and temperature profiles (bottom) for Tr = - 300, at time $21.0 \le t \le 25.4$.

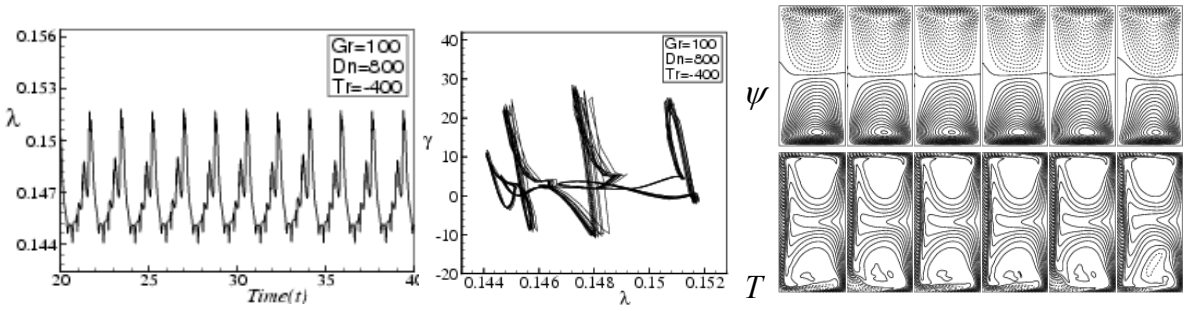

(a) (b) (c)

Figure 7: (a) Time evolution of λ for Tr = -400 and Dn = 800 at Gr = 100. (b) Phase space for Tr = - 400. (c) Contours of secondary flow patterns and temperature profiles for Tr = -400, at time $20.6 \le t \le 29.9$.

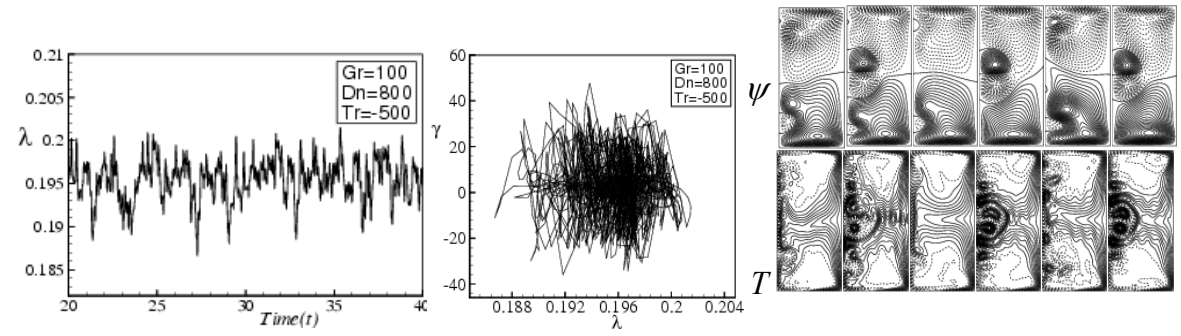

(a) (b) (c)

Figure 8: (a) Time evolution of λ for Tr = - 500 and Dn = 800 at Gr = 100, (b) Phase space for Tr = -500, (c) Contours of secondary flow patterns (top) and temperature profiles (bottom) for Tr = -500 at time $27.0 \le t \le 32.0$.

6. Conclusion

A numerical study is presented for the flow characteristics through a rotating curved rectangular duct of aspect ratio $a = 2$ and curvature $\delta = 0.1$. Numerical calculations are carried out by using a spectral method, and covering a wide range of the Taylor number $-2000 \le Tr < 0$ for the Dean numbers, Dn = 500 and Dn = 800 for the Grashof number $Gr = 100$. We investigated unsteady flow characteristics for the negative rotation of the channel by time evolution calculations, and it is found that the unsteady flow undergoes in the scenario for the case of Dn = 500 is '*steady-state* $\rightarrow$ *multi-periodic* $\rightarrow$ *chaotic'*, and for the case of Dn = 800 is '*Chaotic* $\rightarrow$ *multi-periodic* $\rightarrow$ *periodic* $\rightarrow$ *multi-periodic* $\rightarrow$ *Chaotic'*, if *Tr* is increased in the negative direction. Phase spaces were found to be fruitful to justify the transition of unsteady flow characteristics. Typical contours of secondary flow patterns and temperature profiles are also obtained at several values of *Tr*, and it is found that there exist two- and four-vortex solutions if the duct rotation involved in the negative direction. It is found that the temperature distribution is consistent with the secondary vortices, and convective heat transfer is enhanced as the secondary vortices increase. It is also found that chaotic flow enhances heat transfer more significantly than the periodic or steady-state solutions.

References

1) Nandakumar, K. and Masliyah, J. H. (1986). Swirling Flow and Heat Transfer in Coiled and Twisted Pipes, *Adv. Transport Process*., Vol. **4**, pp. 49-112.

2) Ito, H (1987). Flow in curved pipes. *JSME International Journal*, **30**, pp. 543–552.

3) Yanase, S., Kaga, Y. and Daikai, R. (2002). Laminar flow through a curved rectangular duct over a wide range of the aspect ratio, *Fluid Dynamics Research*, Vol. **31,** pp. 151-183.

4) Selmi, M. and Namdakumar, K. and Finlay W. H., 1994. A bifurcation study of viscous flow through a rotating curved duct, *J. Fluid Mech.* Vol. **262**, pp. 353-375.

5) Wang, L. Q. and Cheng, K.C., 1996. Flow Transitions and combined Free and Forced Convective Heat Transfer in Rotating Curved Channels: the Case of Positive Rotation *Physics of Fluids*, Vol. **8**, pp.1553-1573.

6) Selmi, M. and Namdakumar, K. (1999). Bifurcation Study of the Flow through Rotating Curved Ducts, *Physics of Fluids*, Vol. **11**, pp. 2030-2043.

7) Yamamoto, K., Yanase, S. and Alam, M. M. (1999). Flow through a Rotating Curved Duct with Square Cross-section, *J. Phys. Soc*. Japan, Vol. **68**, pp. 1173-1184.

8) Mondal, R. N., Alam M. M. and Yanase, S. (2007). Numerical prediction of non- isothermal flows through a rotating curved duct with square cross section, *Thommasat Int. J. Sci and Tech.*, Vol. **12**, No. 3, pp. 24-43.

9) Mondal, R. N., Datta, A. K. and Uddin, M. K. (2012). A Bifurcation Study of Laminar Thermal Flow through a Rotating Curved Duct with Square Cross-section, *Int. J. Appl. Mech. and Engg.* Vol. **17** (2). (In Press).

10) Mondal, R. N., Islam, M. S., Uddin, M. K. and Hossain, M. A. (2013). "*Effects of Aspect Ratio on Unsteady Solutions through a Curved Duct Flow*", Appl. Math. & Mech. (Springer), Vol. **34(9)**, pp. 1-16

11) Mondal, R. N., Islam, Md. Zohurul., and Md. saidul Islam, Editors. Transient Heat and Fluid Flow through a Rotating Curved Rectangular Duct: The Case of Positive and Negative Rotation. Proceedings of the 5th BSME International Conference on Thermal Engineering, (2012), December 21-23; IUT, Dhaka.